A Flexible Patch-Type Strain Sensor Based on Polyaniline for Continuous Monitoring of Pulse Waves

SEHONG KANG[1], (Graduate Student Member, IEEE), VEGA PRADANA RACHIM[1], JIN-HYEOK BAEK[2], SEUNG YONG LEE[3], AND SUNG-MIN PARK[1,2], (Member, IEEE)

[1]Department of Creative IT Engineering (CiTE), Pohang University of Science and Technology, Pohang 37673, South Korea
[2]School of Interdisciplinary Bioscience and Bioengineering (IBIO), Pohang University of Science and Technology, Pohang 37673, South Korea
[3]Materials Architecturing Research Center, Korea Institute of Science and Technology, Seoul 126-791, South Korea

Corresponding author: Sung-Min Park (sungminpark@postech.ac.kr)

ABSTRACT A flexible, patch-type strain sensor is described for continuous monitoring of pulse waves. The proposed sensor exploits the piezo-resistivity of the conductive polymer, polyaniline (PANI), to detect dynamic volume changes in blood vessels owing to pulse waves. The proposed PANI film was fabricated through electrodeposition, which is considered as a suitable low-cost technique for mass production in the sensor manufacturing industry. Thus, it is prospective for a disposable wearable sensing system solution in remote healthcare applications. Besides, a flexible sensor packaging can be achieved by laminating the PANI films and an ECOFLEX elastomer to the film bandage. The proposed PANI sensor has high sensitivity (gauge factor of 74.28) and linearity ($R^2 = 0.99$). It also showed a high correlation with commercially available photoplethysmography (PPG) sensor with the small bias and confidence interval to the PPG sensor: bias < 0.1% and confidence interval < 3% for all subjects. Moreover, the proposed PANI sensor was tested for prospective circulatory system-related applications such as measuring heart rate, stiffness index, and pulse transit time. Finally, the proposed study suggests that the proposed PANI sensor is a promising candidate for continuous, long-term, unobtrusive pulse wave monitoring, which can provide real-time insights into an individual's health status.

INDEX TERMS Conductive polymer, flexible sensor, healthcare device, health monitoring, piezoresistive sensor, wearable sensor.

I. INTRODUCTION

The rapid advancement of healthcare electronics has generated particular interest in developing a pulse wave monitoring system that can provide multiple information relating to an individual's cardiovascular health. Pulse waves are periodic arterial pressure signals due to blood circulation. It is closely related to the physiological status, including age, gender, and physical conditions [1]. In addition, it provides key information related to the circulatory system, such as heart rate, blood pressure, stiffness of the artery, and signs of cardiovascular disease [2]–[4]. Therefore, continuous monitoring of pulse

wave facilitates management and early detection of cardio-vascular diseases [5]–[8].

A variety of pulse wave sensors have been developed to continuously collect pulse wave data during a subject's daily life [9], [10]. While sensors based on optics (photoplethysmography (PPG)), ultrasound, and tonometry are commercially available, there remain multiple challenges for robust continuous monitoring. First, PPG monitors vascular pulsation by measuring the intensity of light transmitted through or reflected from a tissue [5]. It is widely used for pulse wave monitoring, but the accuracy of the sensor is affected by the contact between the PPG probes and the tissue [11], [12]. Therefore, commercial PPG sensors are deployed with clamps or straps, which cause discomfort and irritation during

The associate editor coordinating the review of this manuscript and approving it for publication was Srinivas Sampalli.

continuous use. Moreover, the contact changes every time the sensor is worn because it is affected by the tightness of the strap or clamp. Ultrasound pulse wave sensors detect fluctuations in the vessel by penetrating the skin. However, they involve rigid and bulky imaging probes [13], which limit their use as wearable devices that can be used in daily life settings. Among the methods highlighted above, tonometry is the most conventional method to monitor pulse waves. However, the tonometric method requires supporting and pressing structures to flatten a vessel during measurement, using pressure or strain sensors [14], [15]. Such supporting structures, which create force and rigid components of the devices, limit their usability for continuous monitoring. Furthermore, tonometers need to be placed precisely at the center of the artery; the accuracy of the sensor varies with the position in millimeters [7]. These pulse wave sensors have the drawbacks that it is challenging to maintain contact for prolonged use and to wear without obstruction. Therefore, there is a strong clinical need for thin and flexible structures with improved contact for pulse wave sensors for continuous, unobtrusive monitoring in daily life to increase the comfort of the user [16].

Flexible electronics can revolutionize healthcare services with truly comfortable and continuous bio-signal assessments [17]–[20]. Over the past years, flexible and wearable pulse wave sensors have been suggested with the development of flexible electronic technologies. For example, sensors fabricated by blending or laminating conductive particles on flexible substrates were introduced [21], [22]. Although these sensors are flexible and wearable, they are still bulky (2–3 mm thick). Several studies have demonstrated the effectiveness of conductive polymer films as sensing elements for thin and highly sensitive strain sensors for pulse wave monitoring. A graphene-woven fabric-based strain sensor used for pulse wave monitoring under different conditions for people of different ages was demonstrated [23]. While some tradeoff was made between linearity and sensitivity to obtain optimal pulse wave shapes, the flexible sensor showed a gauge factor (GF) of approximately 20. Moreover, thin and flexible strain sensors based on elastomeric/graphene platelet composite films were demonstrated and can significantly increase the GF of up to 150 in 26% strain [24]. The sensor detected pulse waves formed with percussion wave and descending limb wave. However, mass production and uniformity of these sensors are practically limited by their complicated fabrication process, involving high temperature and regulated gas flow.

In this study, we proposed a patch-type pulse wave sensor using the conductive polymer, polyaniline (PANI), which offers high flexibility, ease of fabrication, and long-term operation under daily life conditions. The main fabrication process of the proposed sensor is based on the electrodeposition, which is an established method for mass production that is highly utilized in the circuit manufacturing industry [25]. The proposed sensor is suitable for daily life use because it can be easily attached to the skin without supporting structures while offering high linearity and sensitivity for pulse
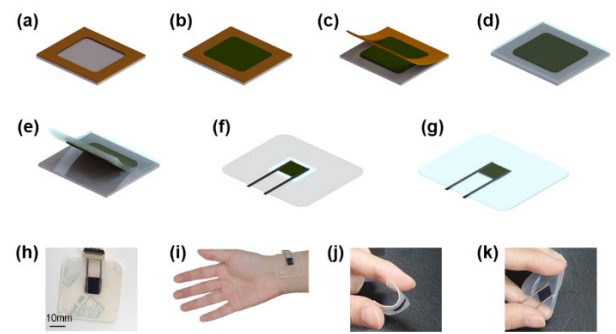
FIGURE 1. Fabrication process for the PANI sensor and its optical image. (a) Masking sheet adhesion. (b) PANI deposition through electrochemical synthesis. (c) Removing the masking sheet. (d) ECOFLEX coating on the PANI layer. (e) Peeling off the ECOFLEX-PANI layer. (f) Connecting silver fabric electrodes. (g) Laminating on bandage and insulating with ECOFLEX. (h) Optical image of the PANI sensor, (i) Wearing, (j) Bending, and (k) Stretching the PANI sensor.

wave monitoring. In previous researches, wearable pulse wave sensors that can be mass-produced were also suggested [26]–[28], but the performance of the proposed sensors or characteristic behavior of the measured pulse wave was not compared against the golden standard device such as commercially available PPG sensor. In this study, we performed comprehensive performance testing to demonstrate the sensor capability for practical application. We analyzed the feature of pulse wave signals to get clinical information. Important parameters for diagnosing health status, such as heart rate, stiffness index, and pulse transit time (PTT) can be extracted and calculated from the feature analysis. The sensor's peak-to-peak time (PT) and heart rate were compared with those of the commercial PPG sensor and the parameter from proposed sensor showed high agreements with the PPG sensor.

The significance of the study can be summarized as follows: (1) a patch-type flexible and wearable pulse wave sensor that can be used in daily life is developed, (2) the proposed sensor can be fabricated by mass-producible method, and (3) the comprehensive testing demonstrates excellent performance of the proposed sensor when compared with the commercially available PPG sensor.

II. METHODS
A. FABRICATION OF PANI SENSOR
The flexible sensor was fabricated on silicone through electrochemical synthesis and layer lamination of the elastomer (Ecoflex-0030, smooth-on) and bandage (3M tegadermTM), as demonstrated in Figure 1a–g. A PANI layer was fabricated using a three-electrode cell. The carbon electrode was used as a counter electrode, whereas the Ag/AgCl electrode was used as a reference electrode.

The working electrode consists of stainless steel plate covered with a masking sheet containing a square hole (Figure 1a). PANI was electrochemically synthesized by chrono potentiometry (Figure 1b). The solvent used was 2N-sulfuric acid (Duksan); 3-ml aniline monomer (Sigma-Aldrich) was

added to 100 ml of electrolyte solution and stirred for 1 h. PANI was electrochemically deposited through chrono potentiometry at a current density of 6.25 mA/cm2 for 10 min. The PANI layer was dried in an oven with the masking sheet removed (Figure 1c), and aggregated; hence, the thickness of the sensor decreased after the drying process. The PANI layer was spin-coated with ECOFLEX substrate, cured in an oven at 60°C for 30 min, and subsequently cooled to room temperature (Figure 1d). The PANI layer-bonded silicone elastomer was carefully peeled off from the working electrode (Figure 1e) and immersed in the dopant acid with different concentrations laminated on a film bandage; 3M tegadermTM was used because of its advantages, including the high adhesion of the film in moist conditions, high conformance to the body, and easy flex with the skin. Silver fabric strips were attached in parallel to both edges of the PANI layer with silver glue as an electrode. The layer and electrodes were then covered and insulated with ECOFlex elastomer (Figure 1f, g). The PANI layer has a thickness of 60 μm, and the ECOFlex coating at both its sides was 360 μm. The silver fabric electrodes were attached to the flexible polyethylene terephthalate (PET) film substrate and connected to the measuring system through a flexible printed circuit connector (Figure 1h) and sheet resistance of the sensor is 200 Ω/sq. The sensor can be attached directly to the skin using the 3M bandage at the bottom of the sensor (Figure 1i). The fabricated sensor was thin (thickness: 800 μm), light (weight: 82 g), and flexible (Figure 1j). The elastic nature of substrates makes the PANI sensor stretchable (Figure 1k) and reduces the shear stress on the skin.

B. CHARACTERIZATION AND OPTIMIZATION OF PANI SENSOR

The morphologies of the surface of the polymer layer were characterized using a field emission scanning electron microscope (FE-SEM, JSM-7800F Prime, JEOL Ltd.). Raman spectra of the polymer layer with different doping concentrations were obtained by inVia Raman microscope (Renishaw) with a laser excitation wavelength of 633nm. We conducted tensile, hysteresis, and fatigue tests using customized stretching machine. The electromechanical response was measured using a potentiostat (Wizmac) under 1 V bias. For optimization, the characteristics and electromechanical response of PANI sensors with different PANI layers were compared. The PANI layers were doped with different concentrations of dopant solution (2M, 1M, 0.25M, and 0.125M sulfuric acid). Five sensors were measured three times for each concentration.

C. PULSE WAVE MONITORING

Pulse wave monitoring of the pre- and post-exercise states were conducted at the Pohang University of Science and Technology in compliance with the human research protocol (PIRB-2018-A001) approved by the POSTECH Institutional Review Board. The subjects attached the PANI sensor to their right wrist and placed the PPG sensor (BIOPAC) on the tip

of their right index finger. They rested for 5 min; after this, their pulse wave is simultaneously measured for 2 min using a sampling frequency of 1 kHz. The subjects then rested again for 5 min, followed by an exercise (jumping jack) for 2 min. After the exercise, the pulse wave of the subject is measured for 2 min. All pulse wave signals were measured with both arms supported and the subjects in a sitting posture.

III. RESULTS AND DISCUSSION
A. WORKING PRINCIPLE OF PANI SENSOR

The proposed PANI sensor is a strain sensor that measures pulse waves by detecting skin deformations. Figure 2a shows the pulse wave monitoring process of the sensor. Blood vessels, including peripheral vessels, periodically contract and expand owing to alternating blood volume flow in the circulatory system [29]. The volume change deforms a layer of skin covering the vessel; thus, the deformation is transferred to the strain on the PANI sensor attached to the skin. The change in strain changes the dynamic resistance of the sensor. The working mechanism of the sensor is illustrated in Figure 2b. As the volume of vessels increases, the strain on the PANI sensor increases as the heart moves to the systole phase. The elongation of the sensor reduces the contact between polymer chains of the PANI sensor because of the shape change and micro-cracks, thereby increasing the resistance of the sensor [26], [30]–[32]. Hence, the resistance of the PANI sensor reflects a pulse wave (the resistance incFreases in the systole phase and decreases in the diastole phase). The pulse wave signals can be monitored by measuring the resistance of the PANI sensor. A suggested wearable system for the sensor is presented in Figure 2c.

B. CHARACTERIZATION OF PANI SENSOR

The morphology of the surface of the PANI layer on the silicone elastomer after doping is shown in Figure 3a. Wrinkling patterns are observed on the PANI film. The wavelength of wrinkling patterns can be changed depending on the concentration of the doping solution, and the film can be dewrinkled by immersing it in a basic solution [33]. The wrinkling patterns and change in the wavelength of the patterns are obtained on the surface of the PANI layers doped with different concentrations of dopant solution (2M, 1M, 0.25M, and 0.125M, see Figure S1).

The resonance Raman spectra of the PANI layer show band appearing in the wave number range 1100–1600 cm^{-1} (Figure 3b). The peak observed at 1586 cm^{-1} is assigned to the C $=$ C stretching vibration in the quinonoid ring [34]. The peak at 1500 cm^{-1} can be assigned to C $=$ N vibration in quinoid rings owing to the depolarization of PANI [35]. The peak at 1339 cm^{-1} is related to the carrier vibration in C–N + delocalized polaronic structures [34], [35]. The band at 1260 cm^{-1} can be connected to benzene-ring deformation vibrations [34]. The peak at 1166 cm^{-1} is related to C–H vibrations of aromatic rings [34], [36]. The band from 1000 to 400 cm^{-1} provides information about in-plane and
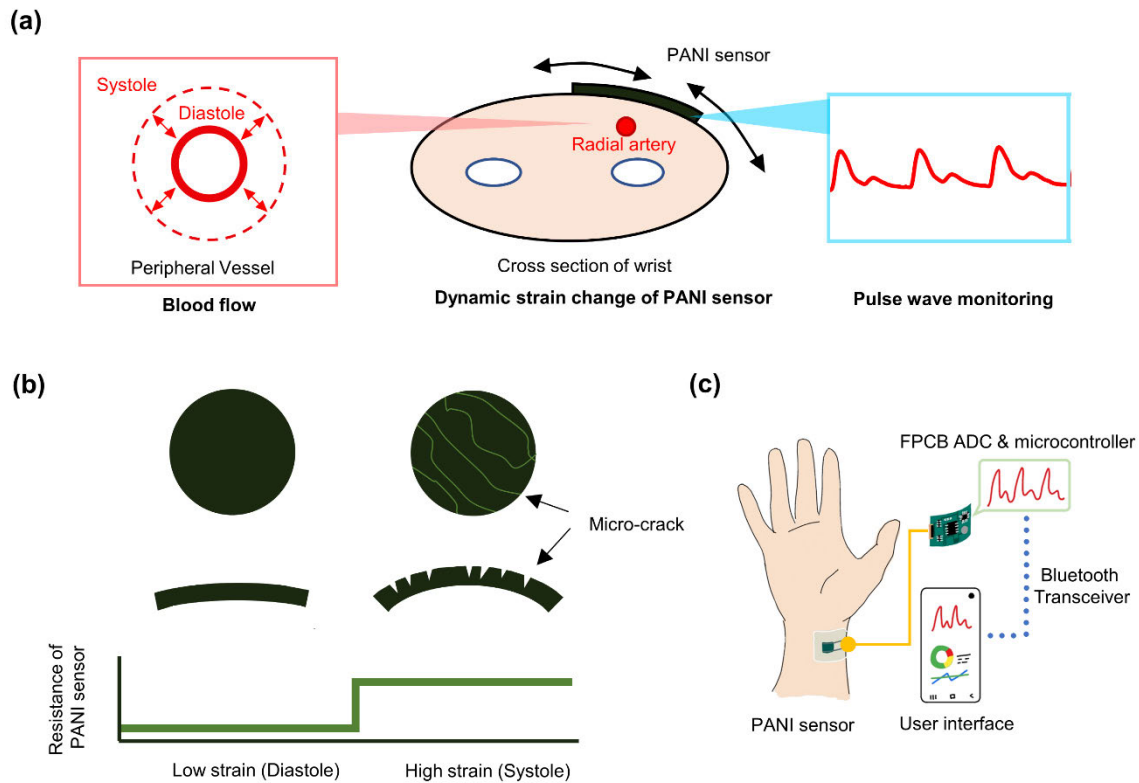
FIGURE 2. Pulse wave monitoring process and system design of wearable PANI sensor. (a) Schematics of the pulse wave monitoring process of the PANI sensor. (b) schematic of the principle of electromechanical response of the PANI sensor. (c) schematic structure of suggested wearable pulse wave monitoring system of the PANI sensor.

out-of-plane vibrations of amine deformation and ring of the PANI structure [36]. Raman spectra and shift of the PANI layers doped with different concentrations of dopant solution are displayed in Figure S2.

C. ELECTROMECHANICAL RESPONSE AND OPTIMIZATION OF PANI SENSOR

The sensitivity and linearity of the sensor is essential for pulse wave sensors. A pulse wave sensor with high sensitivity offers accurate shape of the measured pulse wave as extracting the details of characteristic points of the wave is related to the accuracy of the clinical information estimated from the pulse waves. Linearity assures electrical output change, which is highly correlated with amplitude change of alternating blood pressure and it provides accurate relative position of each characteristic point and shape of pulse waves. Therefore, vital information, such as reflection index, stiffness index, and augmentation index, calculated by the ratio between amplitudes of peaks of pulse wave can be extracted by high sensitivity and linearity. In this work, we assessed the effect of the concentration of dopant solution on the linearity and sensitivity of the pulse wave sensor. The sensitivity of the PANI sensor was evaluated using the $GF = (\Delta R/R0)/\varepsilon$, where R, R0, and ε represent the resistance, rest value of the resistance, and strain of the sensor, respectively. Figure 4 illustrates the elec-

tromechanical response of the proposed sensors composed of PANI layers doped with different concentrations of dopant solution. The electrochemical responses of the four different sensors showed that the linearity increases by increasing the concentration of dopant solution (Figure 4 a, Table 1). The GF of the sensor decreases by increasing the concentration (Figure 4 a, Table 1); however, the GF of PANI sensor doped with 1M dopant solution was higher than the sensor doped with 0.25M dopant solution by up to 0.5% strain. Therefore, we select the sensor doped with 1M dopant solution, and the proposed PANI sensor doped with 1M dopant solution showed both high sensitivity (GF = 74.28) and linearity (R^2 = 0.99) of up to 1% strain. The maximum electrical output for one pulse cycle from the radial artery resulted in approximately 0.25% strain change under the pre-exercise condition and approximately 0.5% strain change under post-exercise conditions. The maximum amplitude from PANI sensor was approximately a quarter of the linear strain range (0%–1.8%), implying that the output signal from the radial artery pulse waves changes within the linear range of the sensor (Figure 4b). The GF and linearity of the sensor is affected by the thickness of the elastomer layer. Both tend to increase as the thickness of the layer decreases (Figure S3). PANI sensor with thin elastomer layers have higher linearity and sensitivity, but they are prone to failure from external

(a)

(b)
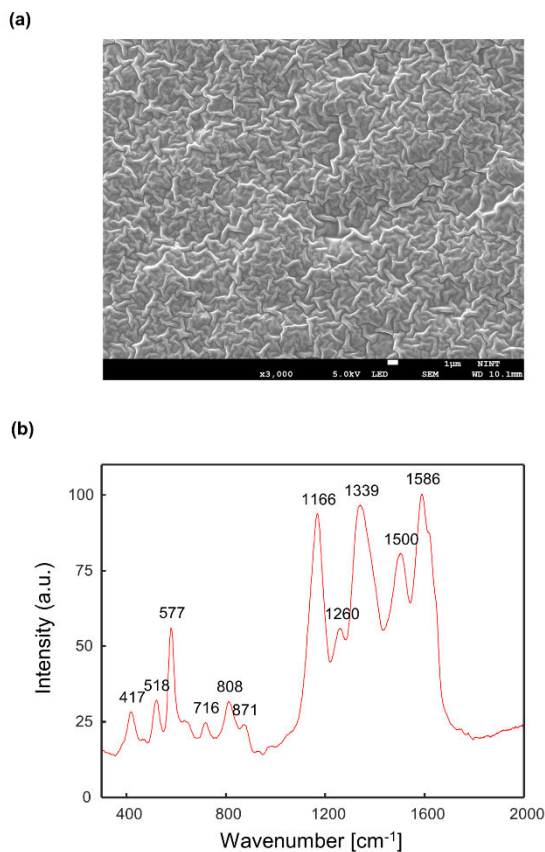
FIGURE 3. Characteristics of PANI layer of the proposed sensor. (a) A field emission scanning electron microscope (FE-SEM) image of the PANI layer morphology, 1 μm. (b) Raman spectrum of the PANI layer.

interferences, including activities related to placing the sensor for measurements, such as attaching or peeling it off the skin. We selected PANI sensor coated with a 360-μm thick ECOFLEX layer, which is relatively robust and has both high linearity and high sensitivity. For pulse wave measurement, maintaining the electromechanical property is important during the expansion, contraction, and repetitive strain cycles. Figure S4 A shows the hysteresis of the proposed sensor under 0%–3% strain repeated five times. The sensor has a similar electromechanical property under both expansion and contraction tensile strains. (Figure S4 A) Figure S4B shows the relative resistance change of the proposed sensor when 0%–0.3% strain is repeated for 3000 cycles. The PANI sensor exhibited higher sensitivity than the reported strain pulse wave sensors (GF of 16.2 [37], 20[23]), which have high linearity of $R^2 = 0.97$. The sensitivity can be increased without reducing the thickness of the elastomer layer by modifying the geometric design of the PANI layer.

D. PULSE WAVE FEATURE ANALYSIS

We evaluated the designed sensor against the reference PPG sensor by comparing the features of the pulse waves measured with both sensors. Figure 5a shows raw data from pulse

(a)

(b)
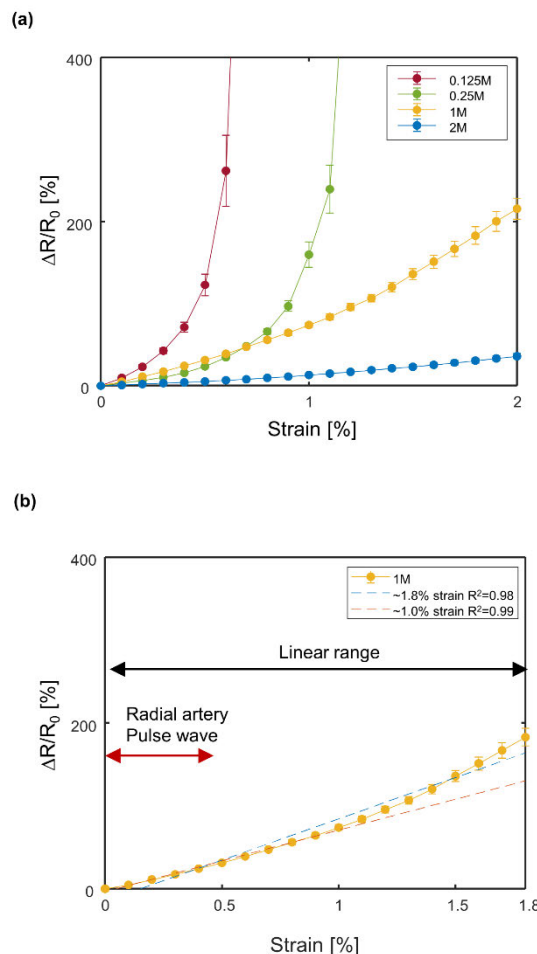
FIGURE 4. Electromechanical response of the PANI sensor under tensile strain. (a) electromechanical response up to 2% strain of the four PANI sensors doped with different concentration of dopant solution. (b) electromechanical response up to 1.8% strain of the proposed PANI sensor.

TABLE 1. Electromechanical properties of PANI sensors doped with different concentrations of dopant solution.

Electromechanical property(~1% strain)	Concentration of dopant solution			
	2M	1M	0.25M	0.125M
Sensitivity (GF)	12.88	74.28	131.43	3617.22
Linearity (R^2)	0.99	0.99	0.79	0.66

waves collected from a subject (a 21-year-old male) at rest over 2 min. Post-exercise pulse wave from the same subject was also collected to evaluate the capability from changes in the feature of the pulse wave after exercise. One hundred continuous pulses from the pulse wave signals were separated by the notch of the pulses. The pulses were overlapped and averaged to identify the characteristic points and features of radial pulse waves. The characteristic points of radial
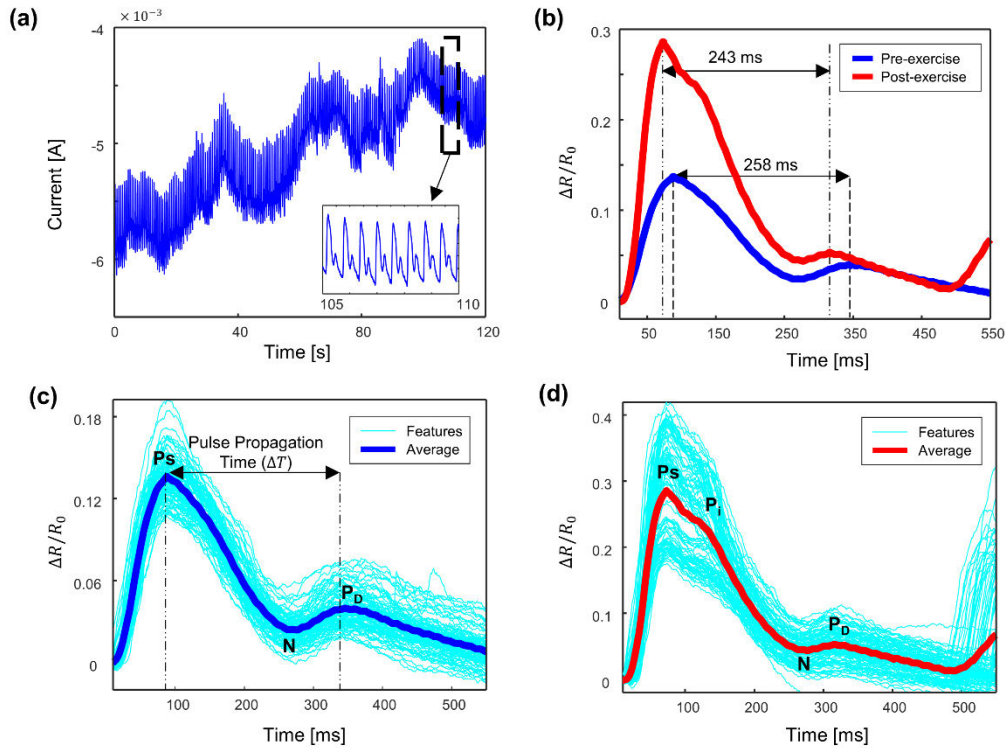
FIGURE 5. Pulse wave feature analysis. (a) Recorded pre-exercise pulse waves from a 21-year-old male subject; inset shows the detailed pulse waves. (b) Overlapped feature and pulse propagation time of averaged pre-and post-exercise pulse. (c)All pulses (cyan) for 2 min, averaged pulse (blue) and three characteristic points of the pre-exercise pulse, and (d) post-exercise.

TABLE 2. Bias and 95% confidence intervals of PT_{PANI} against PT_{PPG} for all subjects.

Parameter (%)	Subject							overall
	1	2	3	4	5	6	7	
Bias	−0.0114	0.0224	−0.0028	0.0013	0.0899	0.0508	0.0421	0.0274 ± 0.04
95% confidence interval	1.9829	2.3139	2.0059	1.6888	2.0760	2.7477	1.4642	2.040 ± 0.41

pulse waves include a systolic peak P_S, a dicrotic notch N, and a diastolic peak P_D [38]. The three points are clearly distinguishable for both pre- and post-exercise pulse waves (Figure 5c, d). The pulse propagation time ΔT, which represents the time delay from the PS to the PD, is altered by physiological conditions such as exercise [39]. In other words, ΔT reduces with increased heart rate due to exercise. The averaged post-exercise pulse wave showed shorter ΔT (243 ms) compared with ΔT for the averaged pre-exercise pulse waves (258 ms) (Figure 5b). Moreover, the sensor was able to extract main measures of vascular function, such as reflection index, $R.I.(\%) = P_D / P_S \times 100$ and stiffness index, $S.I. = (\text{subject's height})/\Delta T$ from the data [39], [40]. The R.I. decreased from 29% to 18%, while the S.I increased from 7.05 [m/s] to 7.48 [m/s] after exercising. The point of inflection P_i, which results from the tidal wave, became

distinguishable in the post-exercise pulses, whereas it was indistinguishable in the pre-exercise pulses (Figure 5d). P_i is the peak of the tidal wave (reflected wave). The time difference from the end of the previous pulse (foot) to Pi is related to the arterial stiffness of the entire arterial system [41], [42]. In addition, the augmentation index, which is an indirect measure of arterial stiffness, can be calculated from Pi [43], [44]. The average amplitude of the post-exercise pulse wave increased about two times compared with the pre-exercise pulse. The maximum amplitude pre- and post-exercise was 0.1927 and 0.4194, respectively. This increase in amplitude denotes an increase in the volume of the radial artery that causes the skin to strain. The feature analysis shows that the signal from the sensor had the characteristic features and behavior of pulse waves, and can extract vital indicators related to pulse waves.
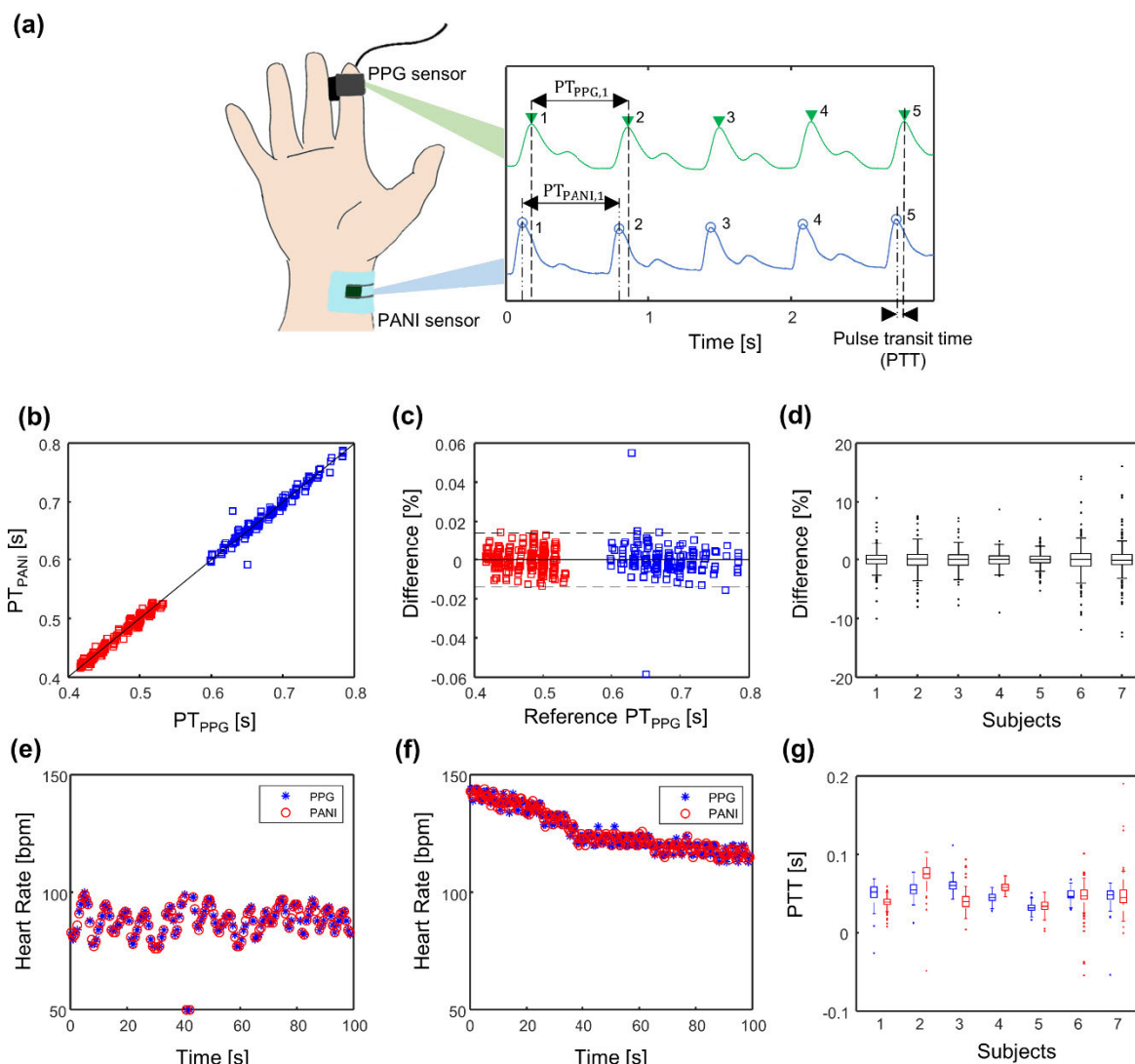
FIGURE 6. Agreement test using PPG sensor and vital indicators extracted from the pulse wave signal. (a) Illustration of agreement test set and pulse wave signal measured by PPG sensor (green) and PANI sensor (blue) (b) Correlation plot, (c) Bland-Altman plot,(d) difference between PT_{PANI} and PT_{PPG} of seven subjects. (e) Representative data of heart rate change from subject 4 calculated from two sensors of pre-exercise (f) post-exercise (g) PTT change between pre-(blue) and post-(red) exercise data of seven subjects.

E. PULSE WAVE MONITORING CAPABILITY TEST UNDER INTERFERENCE CONDITION

Maintaining the capacity to monitor pulse waves under interference, including flexing the wrist, is essential for practical use [23]. The effect of interferences, such as flexing the wrist, on the signal was investigated by recording a pulse wave. The subject attaches the PANI sensor and wears an arm aid designed to flex the wrist at the desired angle. The subject flexes the wrist back and forth for 30°. As demonstrated in Figure S5 A, the resistance (baseline) and resistance change for one pulse cycle increase after flexing owing to additional strain by the motion. Three characteristic peaks were distinguishable during the flexed phase of the motion (Figure S5 B). The resistance and feature of the pulse waves were almost immediately recovered by returning the wrist to the straight condition (0°), so that the three peaks can

be clearly recorded. Thus, the pulse signal was lost only during flexing, and the signal immediately stabilized after the movement, both in the flexed and straight conditions. This result indicates that the motion artifact limits our sensor by potentially reducing the overall signal quality and its ability for clinical analysis. However, it also showed that the stabilization time of the sensor is short (400 ms), which is advantageous in practical use. The motion artifact problem can be solved with further signal processing [44] and with the use of an array PANI sensor. The proposed sensor was fabricated through mask-deposition; thus, an array can be easily obtained by changing the design of the masking sheet. The PANI sensor array may provide redundant pulse wave signals that can be useful for removing the motion artifact without additional sensors, such as accelerometers.

TABLE 3. Heart rate of PANI sensor under pre- and post-exercise condition for all subjects.

Condition	Sensor	Subject						
		1	2	3	4	5	6	7
Pre-exercise	PANI	78.0 ± 4.6	78.1 ± 2.8	81.9 ± 3.0	87.7 ± 7.1	67.5 ± 4.3	76.7 ± 5.6	75.4 ± 4.3
	PPG	77.9 ± 4.2	78.1 ± 2.8	81.9 ± 3.0	87.8 ± 7.1	67.6 ± 4.4	76.7 ± 5.6	75.6 ± 4.8
Post-exercise	PANI	106.0 ± 12.2	117.4 ± 8.8	102.8 ± 15.5	126.7 ± 8.8	93.2 ± 4.1	124.1 ± 9.3	82.6 ± 12.6
	PPG	106.0 ± 12.1	117.3 ± 8.0	102.6 ± 14.8	126.6 ± 8.8	93.5 ± 5.8	124.1 ± 9.2	82.5 ± 12.2

Heart rate (bpm)

TABLE 4. A comparison of the performance of previous strain or pressure sensors with that of the PANI sensor.

Reference	Linearity	Sensitivity [Pulse wave amplitude (GF~1% strain)]	Fabrication techniques or requirements included	Material	Pulse wave test	Peak recognition	Comparison test with commercial pulse wave sensor
This work	0.99	0.1–0.5 (74.28)	Electrodeposition	Polyaniline	Yes	Yes	Yes
[23]	0.97	0.02–0.4 (20)	High temp(>1000□)	Graphene	Yes	Yes	No
[24]	*	0.05–0.09	High temp(>700□)	Graphene	Yes	No	No
[26]	*	(54)	Redox synthesis	Polyaniline	No	No	No
[27]	0.965	(7.492kPa^{-1})	Screen printing	SilverNW, porous cellulose	Yes	Limited	No
[37]	*	0.15 (16.2)	Layer lamination	Reduced graphene film	Yes	No	No
[49]	*	0.09 (33.4)	Laser scribing	self-locked overlapping graphene sheets	Yes	Yes	No
[50]	*	(87)	Electron irradiation	Graphene nano crystallites	No	No	No
[51]	0.999	0.005 (79)	High temp(>200□)	ZnO/graphene nanoplatelets	Yes	Limited	No
[52]	*	0.005 (22.9)	Electrospinning drop-cast	Mxene	Yes	No	No
[53]	0.93	(0.1)	Aerosol jet printing	SilverNW	Yes	Yes	Morphology of pulse only

* Not shown

F. AGREEMENT TEST WITH PPG SENSOR

We evaluated the proposed PANI sensor against a commercial PPG sensor to assess its validity. Seven healthy subjects (3 females and 4 males aged 20–30) were recruited for this test. Each subject attached the PANI sensor on their right wrist and wrapped the PPG sensor to the tip of their right index finger. Continuous pulse wave signals from each sensor were simultaneously recorded before and after the exercise. Pul$_{PANI}$ and Pul$_{PPG}$ are the pulses recorded by PANI and PPG sensors, respectively. Each Pul$_{PANI}$s matched with Pul$_{PPG}$, which has the closest characteristic point from

the same point of the target Pul$_{PANI}$. The P$_S$ from the two sensors were extracted as the characteristic point using a peak detection algorithm; next, Pul$_{PANI}$s was matched with Pul$_{PPG}$s (Figure 6a).PT is peak-to-peak time interval of pulse waves. The PTs of each pulse from the two sensor, PT$_{PANI}$ and PT$_{PPG}$, were calculated and Heart rate (bpm) compared for the matched Pul$_{PANI}$ and Pul$_{PPG}$. Figures 6b, c show the correlation and limits of agreement between PT$_{PANI}$ and PT$_{PPG}$. According to the regression results, the slope of PT$_{PANI}$ versus PT$_{PPG}$ is 0.9965, with R^2 of 0.9956 and mean absolute percentage error of 0.8925%. The mean value of the

bias and the confidence intervals of PT_{PANI} against PT_{PPG} are summarized in Table 2. Subject 5 showed the largest bias of 0.0899%, and subject 4 showed the smallest bias of 0.0013%. The largest confidence interval of 2.3139% was discovered by subject 2, and subject 7 showed the smallest confidence interval of 1.4642%. The bias and the confidence interval for all subjects were under 0.1% and 3% indicating excellent agreement between the PANI and PPG sensors. As shown in Figure 6d, the maximum and minimum difference, excluding outliers for the PT, were within 4%. The outliers may be attributed to the movement of the subject, such as motion of fingers. The PTs were not exactly equal because the two sensors measured PTs from different sites on the body. Both the pre- and post-exercise PT_{PANI} are closely correlated and show agreement with PT_{PPG}. The pre- and post-exercise heart rates were also calculated from PT. The post-exercise PT (red) is lower than the pre-exercise PT (blue) owing to the increase in heart rate after exercise. Figures 6e, f show the calculated continuous heart rate of subject 4 as a function of time under pre- and post-exercise conditions. The pre-exercise heart rate was approximately 90 bpm, while the post-exercise heart rate increased to 145 bpm; then, it gradually fell at a rate of approximately 20 bpm with recovery. Mean of heart rates calculated from PANI sensor and PPG sensor under pre- and post-exercise conditions for all subjects are summarized in Table 3. The differences between the mean heart rates from the two sensors for all subjects were less than 0.3 bpm and the heart rates increased after exercise. Therefore, the proposed sensor showed the characteristic behavior of the heart rate, i.e., an increase in the heart rate during exercise, and can provide continuous heart rate data which has a high agreement between the heart rate of PPG sensor.

Moreover, vital information related to blood pressure and PTT can be collected by comparing the signal from the two sensors. PTT represents the time delay when a pulse travels from the proximal site to the distal site. It has been widely demonstrated and accepted as a key factor for estimating systolic and diastolic blood pressure [46]. P_S of the pulse wave from the Pul_{PANI} was recorded slightly earlier than the peaks from the Pul_{PPG} because the PANI senor measured the pulse waves on the proximal site. Therefore, the PTT between the two sensors was calculated from the data. The mean of the PTT for the pre-exercise recording was 44.7 ± 5.9 ms, while that of the post-exercise PTT was 58.1 ± 5.4 ms. It has been reported that the pulse wave velocity is unaffected by an increase in the heart rate after cumulative exercise [47]. Figure 6g shows the PTT for the seven subjects. It can be seen that exercise did not cause any coherent change in PTT but increased the heart rate. Pulse wave velocity has been used to detect changes in the artery and prognosis of cardiovascular diseases [48]. According to the Moens–Korteweg equation, pulse wave velocity, which depends on the elastic properties of the arteries and blood, is defined as the ratio of the length of the vessel to the PTT[45]. Assuming that the distance between the two sensors is the vessel length, the pulse wave velocity can be calculated using the measured

distance between the sensors and PTT. From these results, the series of sensors attached along the blood vessel can provide cuff-less blood pressure estimation by measuring indicators such as pulse wave velocity.

G. PERFORMANCE COMPARISON ANALYSIS

Table 4 shows the advantages of the proposed wearable pulse wave sensor compared against those of other wearable strain or pressure sensors from other studies.

Both linearity and sensitivity of the sensor are essential for pulse wave monitoring (III Result and discussion, *C.*). However, the linearity of the sensor has not been investigated in most of the previous researches. Our proposed sensor demonstrates linearity of 0.99 and sensitivity of 74.28, which are comparable or superior to the existing sensors. Moreover, we also utilize a cost-efficient material and mass-producible fabrication technique. Utilization of graphene and high temperature-based technique are time consuming and cost inefficient, thus may not be suitable for commercialization [23], [24], [37], [49]–[51]. In some other works [27], [53], researchers utilized a screen printing technology, which is also suitable technique for commercialization. However, the SilverNW is considered as an unaffordable material for sensor fabrication, specifically for disposable-pulse wave sensing system.

In addition, we evaluated our proposed sensor with validation experiment including pulse wave feature analysis and agreement test to the commercialized PPG device. Although evaluating the overall sensor capability in practical application is important, these analyses have not been investigated in most of the previous studies as seen in the Table 4. The results of the analyses indicated that our low-cost, flexible, and wearable pulse wave sensor (1) can provide vital information related to the cardiovascular health, (2) can be fabricated with mass-producible method and cost-efficient material, and (3) can be used as a true continuous plethysmography monitor for real world application.

IV. CONCLUSION

A flexible, wearable strain sensor based on the piezo-resistivity of the PANI was developed for continuous pulse wave monitoring. The proposed sensor employs low-cost materials and simple manufacturing processes; hence, it has high application prospects as a disposable and inexpensive sensor. Three characteristic points were distinguishable for both pre- and post-exercise output signals, thus providing vital information related to the circulatory system. Further, the output signals from the sensor were highly correlated with the signals from commercial PPG sensor. A limitation of the designed sensor is that its operation is affected by motion artifacts. This can be improved through signal processing and post-correction using reference data from multi-sensor arrays because the sensor rapidly stabilizes when the movement ends. The sensor achieves high linearity and sensitivity by setting desired doping conditions and sensor thickness for pulse wave monitoring applications. We expect that the sensor can

be used in other medical application, such as monitoring motion, carotid pulse wave, and respiratory by controlling the sensitivity and linearity of the sensor. In conclusion, our proposed sensor can be used as a flexible, unobtrusive medical device for continuous monitoring of cardiovascular activity.

REFERENCES

[1] J. Yang, J. Chen, Y. Su, Q. Jing, Z. Li, F. Yi, X. Wen, Z. Wang, and Z. L. Wang, "Eardrum-inspired active sensors for self-powered cardiovascular system characterization and throat-attached anti-interference voice recognition," *Adv. Mater.*, vol. 27, no. 8, pp. 1316–1326, Feb. 2015, doi: 10.1002/adma.201404794.

[2] S. Hodis and M. Zamir, "Pulse wave velocity as a diagnostic index: The pitfalls of tethering versus stiffening of the arterial wall," *J. Biomech.*, vol. 44, no. 7, pp. 1367–1373, Apr. 2011, doi: 10.1016/J.JBIOMECH.2010.12.029.

[3] C. Regan, H. Regan, P. Fanelli, and F. Sannajust, "Getting more from blood pressure signals: Use of pulse wave analysis (PWA) to enable greater insight to compound-dependent hemodynamic effects," *J. Pharmacol. Toxicol. Methods*, vol. 99, Sep. 2019, Art. no. 106595, doi: 10.1016/J.VASCN.2019.05.122.

[4] E. von Wowern, K. Källén, and P. Olofsson, "Arterial stiffness in normal pregnancy as assessed by digital pulse wave analysis by photoplethysmography—A longitudinal study," *Pregnancy Hypertension*, vol. 15, pp. 51–56, Jan. 2019, doi: 10.1016/J.PREGHY.2018.11.002.

[5] M. Elgendi, R. Fletcher, Y. Liang, N. Howard, N. H. Lovell, D. Abbott, K. Lim, and R. Ward, "The use of photoplethysmography for assessing hypertension," *npj Digit. Med.*, vol. 2, no. 1, p. 60, Dec. 2019, doi: 10.1038/s41746-019-0136-7.

[6] J. P. Lekakis, N. A. Zakopoulos, A. D. Protogerou, T. G. Papaioannou, V. T. Kotsis, V. C. Pitiriga, M. D. Tsitsirikos, K. S. Stamatelopoulos, C. M. Papamichael, and M. E. Mavrikakis, "Arterial stiffness assessed by pulse wave analysis in essential hypertension: Relation to 24-h blood pressure profile," *Int. J. Cardiol.*, vol. 102, no. 3, pp. 391–395, Jul. 2005, doi: 10.1016/J.IJCARD.2004.04.014.

[7] L. Peter, N. Noury, and M. Cerny, "A review of methods for non-invasive and continuous blood pressure monitoring: Pulse transit time method is promising?" *IRBM*, vol. 35, no. 5, pp. 271–282, Oct. 2014, doi: 10.1016/J.IRBM.2014.07.002.

[8] J. Xia and S. X. M. Liao, "Pulse wave analysis for cardiovascular disease diagnosis," *Digit. Med.*, vol. 4, pp. 35–45, 2018, doi: 10.4103/digm.digm_2_18.

[9] D. Castaneda, A. Esparza, M. Ghamari, C. Soltanpur, and H. Nazeran, "A review on wearable photoplethysmography sensors and their potential future applications in health care," *Int. J. Biosensors Bioelectron.*, vol. 4, no. 4, pp. 195–202, 2018, doi: 10.15406/ijbsbe.2018.04.00125.

[10] D. R. Seshadri, R. T. Li, J. E. Voos, J. R. Rowbottom, C. M. Alfes, C. A. Zorman, and C. K. Drummond, "Wearable sensors for monitoring the physiological and biochemical profile of the athlete," *npj Digit. Med.*, vol. 2, no. 1, p. 72, Dec. 2019, doi: 10.1038/s41746-019-0150-9.

[11] H. Hsiu, C.-L. Hsu, and T.-L. Wu, "Effects of different contacting pressure on the transfer function between finger photoplethysmographic and radial blood pressure waveforms," *Proc. Inst. Mech. Eng., H, J. Eng. Med.*, vol. 225, no. 6, pp. 575–583, Jun. 2011, doi: 10.1177/0954411910396288.

[12] J. K. Sim, B. Ahn, and I. Doh, "A contact-force regulated photoplethysmography (PPG) platform," *AIP Adv.*, vol. 8, no. 4, Apr. 2018, Art. no. 045210, doi: 10.1063/1.5020914.

[13] C. Wang *et al.*, "Monitoring of the central blood pressure waveform via a conformal ultrasonic device," *Nature Biomed. Eng.*, vol. 2, no. 9, pp. 687–695, Sep. 2018, doi: 10.1038/s41551-018-0287-x.

[14] M. Kaisti, T. Panula, J. Leppänen, R. Punkkinen, M. J. Tadi, T. Vasankari, S. Jaakkola, T. Kiviniemi, J. Airaksinen, P. Kostiainen, U. Meriheinä, T. Koivisto, and M. Pänkäälä, "Clinical assessment of a non-invasive wearable MEMS pressure sensor array for monitoring of arterial pulse waveform, heart rate and detection of atrial fibrillation," *npj Digit. Med.*, vol. 2, no. 1, p. 39, Dec. 2019, doi: 10.1038/s41746-019-0117-x.

[15] Y. Sun, Y. Dong, R. Gao, Y. Chu, M. Zhang, X. Qian, and X. Wang, "Wearable pulse wave monitoring system based on MEMS sensors," *Micromachines*, vol. 9, no. 2, p. 90, Feb. 2018, doi: 10.3390/mi9020090.

[16] D.-H. Kim, R. Ghaffari, N. Lu, and J. A. Rogers, "Flexible and stretchable electronics for biointegrated devices," *Annu. Rev. Biomed. Eng.*, vol. 14, no. 1, pp. 113–128, Aug. 2012, doi: 10.1146/annurev-bioeng-071811-150018.

[17] M. Chung, G. Fortunato, and N. Radacsi, "Wearable flexible sweat sensors for healthcare monitoring: A review," *J. Roy. Soc. Interface*, vol. 16, no. 159, Oct. 2019, Art. no. 20190217, doi: 10.1098/rsif.2019.0217.

[18] G. Ge, W. Huang, J. Shao, and X. Dong, "Recent progress of flexible and wearable strain sensors for human-motion monitoring," *J. Semicond.*, vol. 39, no. 1, Jan. 2018, Art. no. 011012, doi: 10.1088/1674-4926/39/1/011012.

[19] S. Khan, S. Ali, and A. Bermak, "Recent developments in printing flexible and wearable sensing electronics for healthcare applications," *Sensors*, vol. 19, no. 5, p. 1230, Mar. 2019, doi: 10.3390/s19051230.

[20] A. Nag, S. C. Mukhopadhyay, and J. Kosel, "Wearable flexible sensors: A review," *IEEE Sensors J.*, vol. 17, no. 13, pp. 3949–3960, Jul. 2017, doi: 10.1109/JSEN.2017.2705700.

[21] Y. H. Kwak, W. Kim, K. B. Park, K. Kim, and S. Seo, "Flexible heartbeat sensor for wearable device," *Biosensors Bioelectron.*, vol. 94, pp. 250–255, Aug. 2017, doi: 10.1016/J.BIOS.2017.03.016.

[22] Y.-Z. Zhang, K. H. Lee, D. H. Anjum, R. Sougrat, Q. Jiang, H. Kim, and H. N. Alshareef, "MXenes stretch hydrogel sensor performance to new limits," *Sci. Adv.*, vol. 4, no. 6, Jun. 2018, Art. no. eaat0098, doi: 10.1126/sciadv.aat0098.

[23] T. Yang, X. Jiang, Y. Zhong, X. Zhao, S. Lin, J. Li, X. Li, J. Xu, Z. Li, and H. Zhu, "A wearable and highly sensitive graphene strain sensor for precise home-based pulse wave monitoring," *ACS Sensors*, vol. 2, no. 7, pp. 967–974, Jul. 2017, doi: 10.1021/acssensors.7b00230.

[24] Q. Meng, Z. Liu, S. Han, L. Xu, S. Araby, R. Cai, Y. Zhao, S. Lu, and T. Liu, "A facile approach to fabricate highly sensitive, flexible strain sensor based on elastomeric/graphene platelet composite film," *J. Mater. Sci.*, vol. 54, no. 15, pp. 10856–10870, Aug. 2019, doi: 10.1007/s10853-019-03650-1.

[25] T. M. Braun and D. T. Schwartz, "The emerging role of electrodeposition in additive manufacturing," *Interface Mag.*, vol. 25, no. 1, pp. 69–73, Jan. 2016, doi: 10.1149/2.F07161if.

[26] X. X. Gong, G. T. Fei, W. B. Fu, M. Fang, X. D. Gao, B. N. Zhong, and L. D. Zhang, "Flexible strain sensor with high performance based on PANI/PDMS films," *Organic Electron.*, vol. 47, pp. 51–56, Aug. 2017, doi: 10.1016/j.orgel.2017.05.001.

[27] L. Xie, P. Chen, S. Chen, K. Yu, and H. Sun, "Low-cost and highly sensitive wearable sensor based on napkin for health monitoring," *Sensors*, vol. 19, no. 15, p. 3427, Aug. 2019, doi: 10.3390/s19153427.

[28] L. Wang, Z. Lou, K. Jiang, and G. Shen, "Bio-multifunctional smart wearable sensors for medical devices," *Adv. Intell. Syst.*, vol. 1, no. 5, Sep. 2019, Art. no. 1900040, doi: 10.1002/aisy.201900040.

[29] A. J. Pappano and W. G. Wier, Eds., "The peripheral circulation and its control," in *Cardiovascular Physiology*, 10th ed. Philadelphia, PA, USA: Content Repository Only, 2013, ch. 9, pp. 171–194.

[30] H. Jung, C. Park, H. Lee, S. Hong, H. Kim, and S. J. Cho, "Nanocracked strain sensor with high sensitivity and linearity by controlling the crack arrangement," *Sensors*, vol. 19, no. 12, p. 2834, Jun. 2019, doi: 10.3390/s19122834.

[31] I. A. Rashid, M. S. Irfan, Y. Q. Gill, R. Nazar, F. Saeed, A. Afzal, H. Ehsan, A. A. Qaiser, and A. Shakoor, "Stretchable strain sensors based on polyaniline/thermoplastic polyurethane blends," *Polym. Bull.*, vol. 77, no. 3, pp. 1081–1093, Mar. 2020, doi: 10.1007/s00289-019-02796-x.

[32] Y. Xiao, S. Jiang, X. Zhao, H. Jiang, and W. Zhang, "Crack-enhanced mechanosensitivity of cost-effective piezoresistive flexible strain sensors suitable for motion detection," *Smart Mater. Struct.*, vol. 27, no. 10, Oct. 2018, Art. no. 105049, doi: 10.1088/1361-665X/aadc89.

[33] J. Xie, C. Zong, X. Han, H. Ji, J. Wang, X. Yang, and C. Lu, "Redox-switchable surface wrinkling on polyaniline film," *Macromolecular Rapid Commun.*, vol. 37, no. 7, pp. 637–642, Apr. 2016, doi: 10.1002/marc.201500700.

[34] J. Stejskal, M. Trchova, P. Bober, P. Humpolicek, V. Kasparkova, I. Sapurina, M. A. Shishov, and M. Varga, "Conducting polymers: Polyaniline," in *Encyclopedia of Polymer Science and Technology*, 4th ed. Hoboken, NJ, USA: JWS, Jun. 2015, pp. 1–44, doi: 10.1002/0471440264.pst640.

[35] G. M. do Nascimento and M. L. A. Temperini, "Studies on the resonance Raman spectra of polyaniline obtained with near-IR excitation," *J. Raman Spectrosc.*, vol. 39, no. 7, pp. 772–778, Jul. 2008, doi: 10.1002/jrs.1841.

[36] A. B. Rohom, P. U. Londhe, S. K. Mahapatra, S. K. Kulkarni, and N. B. Chaure, "Electropolymerization of polyaniline thin films," *High Perform. Polym.*, vol. 26, no. 6, pp. 641–646, Sep. 2014, doi: 10.1177/0954008314538081.

[37] Q. Liu, J. Chen, Y. Li, and G. Shi, "High-performance strain sensors with Fish-Scale-Like graphene-sensing layers for full-range detection of human motions," *ACS Nano*, vol. 10, no. 8, pp. 7901–7906, Aug. 2016, doi: 10.1021/acsnano.6b03813.

[38] C. Fischer, M. Glos, T. Penzel, and I. Fietze, "Extended algorithm for real-time pulse waveform segmentation and artifact detection in photo-plethysmograms," *Somnologie*, vol. 21, no. 2, pp. 110–120, Jun. 2017, doi: 10.1007/s11818-017-0115-7.

[39] A. Wang, L. Yang, W. Wen, S. Zhang, D. Hao, S. G. Khalid, and D. Zheng, "Quantification of radial arterial pulse characteristics change during exercise and recovery," *J. Physiol. Sci.*, vol. 68, no. 2, pp. 113–120, Mar. 2018, doi: 10.1007/s12576-016-0515-7.

[40] C.-L. Choong, M.-B. Shim, B.-S. Lee, S. Jeon, D.-S. Ko, T.-H. Kang, J. Bae, S. H. Lee, K.-E. Byun, J. Im, Y. J. Jeong, C. E. Park, J.-J. Park, and U.-I. Chung, "Highly stretchable resistive pressure sensors using a conductive elastomeric composite on a micropyramid array," *Adv. Mater.*, vol. 26, no. 21, pp. 3451–3458, Jun. 2014, doi: 10.1002/adma.201305182.

[41] F. Alaei-Shahmiri, Y. Zhao, and J. Sherriff, "Assessment of vascular function in individuals with hyperglycemia: A cross-sectional study of glucose—Induced changes in digital volume pulse," *J. Diabetes Metabolic Disorders*, vol. 14, no. 1, p. 23, Dec. 2015, doi: 10.1186/s40200-015-0153-2.

[42] S. J. Denardo, R. Nandyala, G. L. Freeman, G. L. Pierce, and W. W. Nichols, "Pulse wave analysis of the aortic pressure waveform in severe left ventricular systolic dysfunction," *Circulat., Heart Failure*, vol. 3, no. 1, pp. 149–156, Jan. 2010, doi: 10.1161/CIRCHEARTFAIL-URE.109.862383.

[43] A. P. Avolio, M. Butlin, and A. Walsh, "Arterial blood pressure measurement and pulse wave analysis—Their role in enhancing cardiovascular assessment," *Physiol. Meas.*, vol. 31, no. 1, pp. R1–R47, Jan. 2010, doi: 10.1088/0967-3334/31/1/R01.

[44] F. Fantin, A. Mattocks, C. J. Bulpitt, W. Banya, and C. Rajkumar, "Is augmentation index a good measure of vascular stiffness in the elderly?" *Age Ageing*, vol. 36, no. 1, pp. 43–48, Nov. 2006, doi: 10.1093/ageing/afl115.

[45] D. Pollreisz and N. TaheriNejad, "Detection and removal of motion artifacts in PPG signals," *Mobile Netw. Appl.*, Aug. 2019, doi: 10.1007/s11036-019-01323-6.

[46] R. Wang, W. Jia, Z.-H. Mao, R. J. Sclabassi, and M. Sun, "Cuff-free blood pressure estimation using pulse transit time and heart rate," in *Proc. 12th Int. Conf. Signal Process. (ICSP)*, Oct. 2014, pp. 115–118, doi: 10.1109/ICOSP.2014.7014980.

[47] R. Kobayashi, H. Hatakeyama, Y. Hashimoto, and T. Okamoto, "Acute effects of accumulated aerobic exercise on aortic and peripheral pulse wave velocity in young males," *J. Phys. Therapy Sci.*, vol. 30, no. 1, pp. 181–184, 2018, doi: 10.1589/jpts.30.181.

[48] A. S. Ferreira, M. A. R. Santos, J. B. Filho, I. Cordovil, and M. N. Souza, "Determination of radial artery compliance can increase the diagnostic power of pulse wave velocity measurement," *Physiol. Meas.*, vol. 25, no. 1, pp. 37–50, Feb. 2004, doi: 10.1088/0967-3334/25/1/004.

[49] D.-Y. Wang, L.-Q. Tao, Y. Liu, T.-Y. Zhang, Y. Pang, Q. Wang, S. Jiang, Y. Yang, and T.-L. Ren, "High performance flexible strain sensor based on self-locked overlapping graphene sheets," *Nanoscale*, vol. 8, no. 48, pp. 20090–20095, 2016, doi: 10.1039/C6NR07620C.

[50] P. Xue, C. Chen, and D. Diao, "Ultra-sensitive flexible strain sensor based on graphene nanocrystallite carbon film with wrinkle structures," *Carbon*, vol. 147, pp. 227–235, Jun. 2019, doi: 10.1016/j.carbon.2019.03.001.

[51] S. Sun, L. Guo, X. Chang, Y. Liu, S. Niu, Y. Lei, T. Liu, and X. Hu, "A wearable strain sensor based on the ZnO/graphene nanoplatelets nanocomposite with large linear working range," *J. Mater. Sci.*, vol. 54, no. 9, pp. 7048–7061, May 2019, doi: 10.1007/s10853-019-03354-6.

[52] K. Yang, F. Yin, D. Xia, H. Peng, J. Yang, and W. Yuan, "A highly flexible and multifunctional strain sensor based on a network-structured MXene/polyurethane mat with ultra-high sensitivity and a broad sensing range," *Nanoscale*, vol. 11, no. 20, pp. 9949–9957, May 2019, doi: 10.1039/C9NR00488B.

[53] R. Herbert, H.-R. Lim, and W.-H. Yeo, "Printed, soft, nanostructured strain sensors for monitoring of structural health and human physiology," *ACS Appl. Mater. Interfaces*, vol. 12, no. 22, pp. 25020–25030, Jun. 2020, doi: 10.1021/acsami.0c04857.

SEHONG KANG (Graduate Student Member, IEEE) received the B.S. degree in mechanical engineering from the Pohang University of Science and Technology (POSTECH), Pohang, South Korea, in 2018, where she is currently pursuing the Ph.D. degree in creative IT engineering. Her current research interests include wearable biosensors, smart soft matter, soft actuators, and their medical application.

VEGA PRADANA RACHIM received the B.Eng. degree in electrical engineering from Diponegoro University, Semarang, Indonesia, in 2012, and the M.Eng. and Ph.D. degrees in electronic engineering from Pukyong National University, Busan, South Korea, in 2015 and 2019, respectively. He is currently a Postdoctoral Researcher Associate with the Department of Creative IT Engineering, Pohang University of Science and Technology (POSTECH), Pohang, South Korea. His current research interests include wearable sensing, multimodal biosensor, biomedical signal processing, and AI for healthcare.

JIN-HYEOK BAEK was born in Busan, South Korea, in April 1991. He received the B.S. degree from the Department of Electronic Engineering, Soongsil University, Seoul, South Korea, in 2015, and the M.S. degree in electrical engineering from the Pohang University of Science and Technology (POSTECH), Pohang, South Korea, in 2017, where he is currently pursuing the Ph.D. degree with the School of Interdisciplinary Bioscience and Bioengineering. His current research interest includes medical device applications.

SEUNG YONG LEE received the bachelor's and master's degrees in materials science and engineering from Seoul National University, in 2000 and 2002, respectively, and the Ph.D. degree in materials science and engineering from the University of Maryland, College Park, in 2012. He is currently a Principal Research Scientist with the Korea Institute of Science and Technology. He has authored or coauthored more than 40 peer-reviewed articles. His research interests include synthesis of nanoparticles and their applications.

SUNG-MIN PARK (Member, IEEE) received the B.S. and Ph.D. degrees in electrical and computer engineering from Purdue University, West Lafayette, IN, USA, in 2001 and 2006, respectively. From 2006 to 2014, he was with Medtronic, Minneapolis, MN, USA, as the Research and Development Manager, leading the award-wining effort in developing the world first MRI conditional pacemaker. From 2014 to 2016, he was with Samsung, Suwon, South Korea, as the Director for spearheading healthcare centric mobile devices and mobile health service platform development projects. He is currently a Professor with the Department of Creative IT Engineering, Pohang University of Science and Technology (POSTECH), Pohang, South Korea, where he has been since 2016.

• • •